Met. Mater. Int., Vol. 15, No. 1 (2009), pp. 107~111
DOI: 10.1007/s12540-009-0107-7 Published 20 February 2009

Magnetic Properties of Vanadium-Doped Silicon Carbide Nanowires

Han-Kyu Seong[1], Tae-Eon Park[1], Seung-Cheol Lee[2], Kwang-Ryeol Lee[2], Jae-Kwan Park[3], and Heon-Jin Choi [1,*]

[1]School of Advanced Materials Science and Engineering, Yonsei University, 134, shinchon-dong, Seodaemun-gu, Seoul 120-749, Korea
[2]Future Technology Research Division, Korea Institute of Science and Technology, 39-1, Hawolgok-dong, Seongbuk-gu, Seoul 136-650, Korea
[3]Material Science and Technology Division, Korea Institute of Science and Technology, Seoul 136-650, Korea

(received date: 9 November 2007 / accepted date: 23 October 2008)

This study reports the magnetic properties of vanadium (V) doped single crystalline silicon carbide nanowires. The first principle calculation indicated that the V-doped cubic SiC phase can exhibit half-metallic ferromagnetic properties that are essential for the realization of spintronic devices. Based on this calculation, V-doped SiC nanowires were fabricated in a chemical vapor deposition process. The single crystalline β-SiC nanowires, which are doped with ca. 4 at.% of V, had diameters of < 100 nm and a length of several μm. High-resolution transmission electron microscopy observations revealed vanadium carbide (VC) phases in the nanowires, even at this low concentration of dopants. Magnetic characterization implies that the nanowires are a mixture of the diamagnetic phase of VC and ferro- or paramagnetic phases of V-doped SiC. These results suggest that the doping of transition metal having high solubility to the SiC phase can lead to the realization of dilute magnetic semiconductor behavior at very low temperature.

Keywords: Silicon carbide nanowires, Doping, Diluted magnetic semiconductor

1. INTRODUCTION

Current information technology relies on two independent processes: charge-based information processing (microprocessors) and spin-based data storage (magnetic hard drives) [1,2]. The perspective of merging these two processes and thus simultaneously manipulating both the charge and spin in a single semiconductor medium leads to the exciting area of spintronics. Among many others, diluted magnetic semiconductors (DMSs), which transform spin-frustrated semiconductors to ferromagnets by magnetic doping, represent the most promising candidates for such applications [3-6]. According to the principle of mean field theory [3], transition metals such as Sc, Ti, V, Cr, Mn, Fe, Co, and Ni with partially filled *d* states can be doped for transforming spin-frustrated semiconductors to ferromagnets. It has also been predicted that room-temperature ferromagnetism, which would be advantageous in many applications, can be achieved in magnetic doped wide band-gap semiconductors [5]. While an in-depth investigation will be done for oxide and III-nitride DMS, other semiconductors such as SiC can also be explored to develop a new class of DMS. Although Mn or Fe implanted *p*-type 6H-SiC thin films have been reported to show the ferromagnetic characteristics with a transition temperature of 250 K [7], the behavior and role of the transition metals in the SiC phases should be addressed in detail. Furthermore, such an implantation process is associated with many defects in the matrix that should be avoided to exploit the DMS properties and further the realization of DMS devices.

Recently, nanowires have been considered as ideal building blocks to address the magnetism in DMSs [8-10]. Nanowires have advantages over thin films with respect to studying magnetism in DMSs. Specifically, they offer thermodynamically stable features and are typically single crystalline and free from defects [11,12]. They can thus safely exclude the effect of defects and non-uniform distributions of dopants that are typically observed in DMSs prepared by non-equilibrium processing (e.g., the molecular beam epitaxial process). The free standing nature of nanowires makes it possible to exclude the effect of thermal and lattice mismatches of the substrate and opens the possibility of determining the intrinsic magnetism under fully relaxed states [13].

*Corresponding author: hjc@yonsei.ac.kr

In a previous study, the authors reported the growth and modulation of undoped SiC nanowires [14,15]. The diameter of SiC nanowires were controlled in the range 20 nm to 50 nm and the wires were vertically synthesized on the substrate by reducing the reactor pressure. Electrical characterization from an individual nanowire indicated that undoped SiC nanowires have n-type semiconductor behavior with a very weak gating effect. These outcomes demonstrated that the SiC nanowires can be modulated by controlling the process condition. On the other hand, the doping process is important to the achievement of reliable building blocks for nanoscale devices, as the one-dimensional nanostructure is an entirely different system compared to bulk or thin film materials. Moreover, transition-metal dopants provide spin magnetic moments associated with their electron spin, meaning that transition-metal doped semiconductors can simultaneously manipulate the charge and spin. In this study, a calculation was made to explore the appearance of ferromagnetism in various semiconductors. It showed that transition metal (Mn, Cr, V) doped semiconductors with cubic structures (e.g., SiC or AlN) can have ferromagnetic and half-metallic properties. Based on this calculation, V-doped SiC nanowires were fabricated and their structures and magnetic properties were characterized.

2. EXPERIMENTAL PROCEDURE

The calculations were performed with the Vienna *Ab initio* Simulation Package (VASP) [16] using the generalized gradient approximation parameterized by Pewdew and Wang [17]. Brillouin zone integration of the self-consistent procedures and the calculations of the total and projected density of states were carried out using the modified tetrahedron method with Blöchl correction [18]. The embedding of impurities into zinc-blende SiC was modeled by a 2 × 2 × 2 supercell formed by eight cubic unit cells. The resulting system contains 64 atoms. The replacement of one Si site with a V atom results in 3 at.% of impurity concentration. The growth of SiC nanowires was carried out in a horizontal hot-wall chemical vapor deposition (CVD) furnace. Oxidized Si/SiO_2 wafers were used as substrates for the growth of SiC nanowires. The substrates, which had a 2 nm layer of Ni deposited by magnetron sputtering, were placed in a region of uniform temperature in an inner quartz tube reactor surrounded by an outer alumina tube. Methyltrichlorosilane (MTS, CH_3SiCl_3) was chosen as a source precursor because it has an equivalent ratio of silicon to carbon and decomposes at a low temperature. H_2 was used as both the carrier gas, which transfers the source precursor through a bubbler to the quartz reactor, and as a diluent gas, which regulates the concentration of the mixture containing the MTS vapor and carrier gas. The diluent and carrier gas, containing MTS vapor, were completely mixed before their introduction to the reactor. Typically, the system was heated to 950 °C under a flow of H_2 at a rate of 1,000 $cm^3 \cdot min^{-1}$ and was maintained for 5 min during which time MTS was added to the flow of H_2 as a carrier gas at a rate of 5 $cm^3 min^{-1}$. It was then cooled to room temperature. To dope V into the nanowires, 0.5 g of solid vanadium chloride (VCl_3) as the doping precursor was positioned upstream at a distance of 5 cm from the substrate.

3. RESULTS AND DISCUSSION

Figure 1 shows the density of state of 3 at.% V-doped SiC. The solid line and gray area indicate the total density of state and vanadium 3 d-like state, respectively. As the spin-up state could be observed at the Fermi level, only V-doped SiC could be regarded as a half metal. The electronic configuration at the Fermi level was dominated by a V 3 d-like band. As the Fermi level is positioned beneath the conduction band of the SiC host, the carriers of the V-doped SiC are likely to be electrons. According to the calculation, the total energy of the magnetic phase was 0.18 eV lower than that of the nommagnetic phase, and the total magnetic moment of the supercell was 1 μ_B (bohr magneton).

Figure 2(a) shows a scanning electron microscopy (SEM) image of SiC nanowires prepared on a substrate under a MTS-H_2 flow. The nanowires were distributed over the entire area of the substrate and have diameters in the range of < 100 nm and a length of several μm. The X-ray powder diffraction (XRD) pattern of the SiC nanowires was indexed to a zinc blend structure β-SiC; the other second phase was not identified. A low-magnification transmission electron microscopy (TEM) observation shows that the nanowires have a

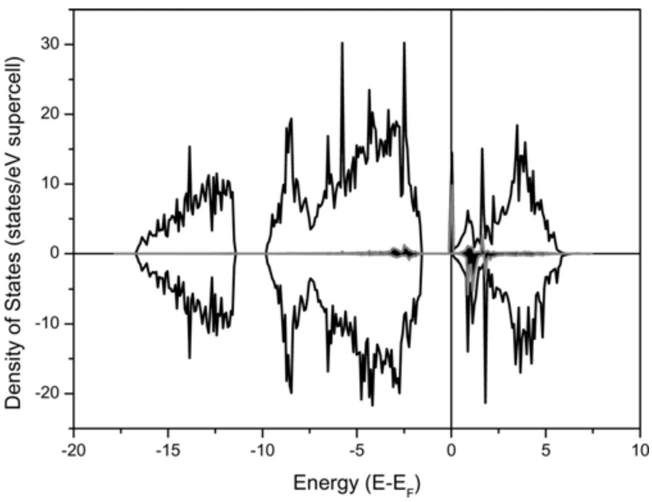

Fig. 1. The total and 3d-metal densities of states of V-doped SiC. The thick solid line and the gray area correspond to the total DOS and 3d-metal projected DOS, respectively. The positive and negative values of the DOS indicate the spin up and spin down state, respectively. The energies of the electron state are plotted with respect to the Fermi energy of the system. Therefore, the Fermi energy was set to zero.

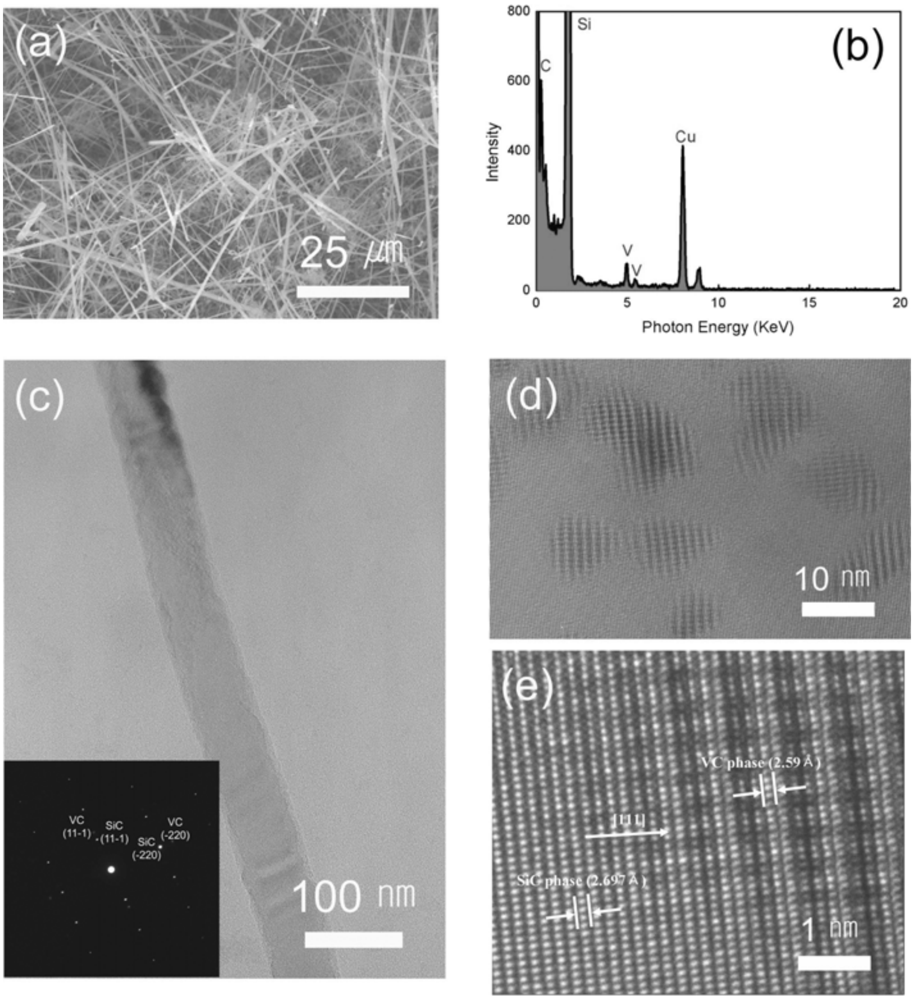

Fig. 2. (a) Typical SEM image of V-doped SiC nanowires grown on substrates. (b) EDS spectrum of a V-doped individual SiC nanowire. (c) TEM image of a V-doped individual SiC nanowire. The inset is a SAED pattern recorded along the [112] zone axis. (d) HR-TEM image of 4 at.% V-doped individual wire. (e) Lattice image of the wire shown in (d).

similar morphology compared to pure SiC nanowires [19]. Selected area electron diffraction (SAED) analysis (inset in Fig. 2(c)), recorded along the [112] zone axis, showed that the nanowires have cubic zinc blend structures with a <111> growth direction. Importantly, the nanowires are nearly perfect single crystalline with little intrinsic defects such as the stacking faults that are observed in bulk or thin film SiC [19]. Furthermore, the free-standing nature of the nanowires on the substrate mitigates the effect of stresses that are generated from the lattice mismatch to the substrate and act as driving forces for the generation of defects. This should contribute to the fabrication of single crystalline SiC nanowires with few defects. Although Ni was used as a catalyst, which clearly contributed to the growth of the nanowires, no Ni or Ni compounds were found in any of the measurements, as the catalysts were etched out by the chloride vapors during the growth of the nanowires in this process. An energy dispersive spectroscopy (EDS) analysis of individual SiC nanowires on TEM indicates the existence of V in the nanowires at approximately 4 at.%, as shown in Fig. 2(b). This indicates that V can be doped into SiC nanowires through this process. Though the second phase was not clearly identified by a XRD or SAED analysis, it was found that the second phase was homogeneously distributed within the SiC lattice (Fig. 2(d)). Figure 2(e) shows a lattice image of nanowires recorded by high-resolution TEM analysis. This image indicates the existence of a second phase in the nanowires with a size of nearly 10 nm. The lattice distance characterization shown in Fig. 2(e) suggests that the second phase is vanadium carbide (VC). The interplanar spacings of the second phases found at the area in Fig. 2(e) were calculated to be 2.59 Å, which corresponds to the interplanar spacings of VC (111), where the SiC matrix was 2.697 Å. This implies that the growth direction of this nanowire is <111>.

The magnetic properties of the nanowires were determined using superconducting quantum interferences device

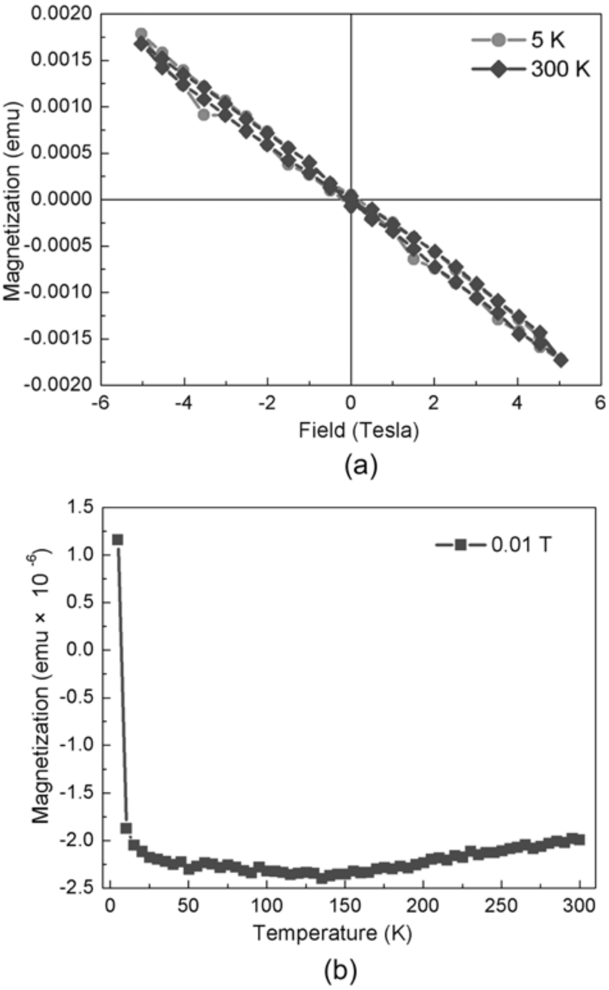

Fig. 3. (a) Magnetization curves of the 6 at.% V-doped SiC nanowires measured at 5 and 300 K. (b) Temperature-dependent magnetization of SiC NW doped with 6 at.% V under a 0.01 T magnetic field.

magnetometry (SQUID). Figure 3(a) shows the magnetization loops of the SiC nanowire sample doped with 4 at.% V. The magnetic data were obtained after an appropriate correction for the diamagnetic component arising from the oxidized silicon substrate. The data indicates that the V-doped SiC nanowires have diamagnetic properties. A literature survey indicates that β-SiC and VC have diamagnetic properties; thus, the observed diamagnetic properties likely originate from the intrinsic magnetic properties of β-SiC and VC. The temperature dependence of the magnetization (Fig. 3(b)) under 0.01 T shows the characteristics of the diamagnetic properties; however, it shows ferromagnetic or paramagnetic behavior below values close to 10 K. Current theoretical and experimental studies indicate that the magnetic ordering of DMS materials is strongly dependent on the amount of magnetic ions. For example, a low concentration of Mn in GaN (e.g., < 1 at.%) results in paramagnetic behavior, whereas higher concentration (e.g., 3 at.%) results in ferromagnetic behavior. The results of this study suggest that much of the V that is doped into the SiC nanowires is consumed as VC; however, a low concentration of V may remain in the matrix, exhibiting weak ferro- or paramagnetic characteristics. Thus, V-doped SiC nanowires may be a mixture of the diamagnetic phase (VC and non-doped β-SiC) and the ferromagnetic or paramagnetic phase (V-doped SiC).

4. CONCLUSIONS

This study investigated V-doped SiC nanowires both theoretically and experimentally. The theoretical result showed that V-doped cubic SiC can exhibit half-metallic and ferromagnetic properties that are essential for realizing spintronic devices. The experimental result indicates that V can be doped into nanowires, which are ideal building blocks for developing nano spintronic devices and represent an ideal single crystalline system to explore a new class of DMS system. The result also suggests that the nanowires consist of diamagnetic and a ferromagnetic or paramagnetic phase due to the low solubility of V to the cubic SiC phase (below ca. 6 %). This implies that the selection and doping of transition metal elements having high solubility to the SiC phase can lead to DMS SiC nanowires at a very low temperature.

ACKNOWLEDGMENTS

This research was supported in part by a grant from the program of the National Research Laboratory of the Korean Ministry of Science and Technology (R0A-2007-000-20075-0), IT R&D program of MKE/IITA (2008-F-023-01, Next generation future device fabricated by using nano junction), the Seoul Research and Business Development Program (10816), Korea Institute of Science and Technology, and the Second Stage of Brain Korea 21 Project in 2007.

REFERENCES

1. S. D. Sarma, *Nature Mater.* **2**, 292 (2003).
2. I. Malajovich, J. J. Berry, N. Samarth, and D. D. Awschalom, *Nature* **411**, 770 (2001).
3. H. Ohno, *Science* **281**, 951 (1998).
4. S. A. Wolf, D. D. Awschalom, R. A. Buhrman, J. M. Daughton, S. von Molnar, M. L. Roukes, A. Y. Chtchelkanova, and D. M. Treger, *Science* **294**, 1488 (2001).
5. T. Dietl, H. Ohno, F. Matsukura, J. Cibert, and D. Ferrand, *Science* **287**, 1019 (2000).
6. J. S. Lee, J. D. Lim, Z. G. Khim, Y. D. Park, S. J. Pearton, and S. N. G. Chu, *J. Appl. Phys.* **93**, 4512 (2003).
7. J. S. Neal, A. J. Behan, R. M. Ibrahim, H. J. Blythe, M. Ziese, A. M. Fox, and G. A. Gehring, *Phys. Rev. Lett.* **96**, 197208 (2006).
8. H. J. Choi, H. K. Seong, J. Chang, K. I. Lee, Y. J. Park, J. J.

Kim, S. K. Lee, R. He, T. Kuykendall, and P. Yang, *Adv. Mater.* **17**, 1351 (2005).

9. H. K. Seong, Y. Lee, J. K. Kim, Y. K. Byeun, K. S. Han, J. G. Park, and H. J. Choi, *Adv. Mater.* **18**, 3019 (2006).
10. H. K. Seong, J. Y. Kim, J. J. Kim, S. C. Lee, S. R. Kim, U. Kim, T. E. Park, and H. J. Choi, *Nano Lett.* **7**, 3366 (2007).
11. H. K. Seong, H. Jeong, R. Ha, J. C. Lee, Y. M. Sung, and H. J. Choi, *Met. Mater. Int.* **14**, 353 (2008).
12. H. K. Seong, M. H. Kim, H. J. Choi, Y. J. Choi, and J. G. Park, *Met. Mater. Int.* **14**, 477 (2008).
13. N. Thillosen, K. Sebald, H. Hardtdegen, R. Meijers, R. Calarco, S. Montanari, N. Kaluza, J. Gutowski, and H. Luth, *Nano Lett.* **6**, 704 (2006).
14. H. J. Choi, H. K. Seong, J. C. Lee, and Y. M. Sung, *J. Crys. Growth* **269**, 472 (2004).
15. H. K. Seong, S. K. Lee, H. J. Choi, J. I. Lee, and D. J. Choi, *Appl. Phys. Lett.* **85**, 1256 (2004).
16. G. Kresse, and J. Furthmuller, *Comput. Mater. Sci.* **6**, 15 (1996); *Phys. Rev. B* **54**, 11169 (1996).
17. J. P. Perdew, J. A. Chevary, S. H. Vosko, K. A. Jackson, M. R. Pederson, D. J. Singh, and C. Fiolhais, *Phys. Rev. B* 46, 6671 (1992); Y. Wang, and J. P. Perdew, *Phys. Rev. B* **44**, 13298 (1991).
18. P. E. Blochl, *Phys. Rev. B* **50**, 17953 (1994).
19. C. Hallin, A. O. Konstantinov, B. Pecz, O. Kordina, and E. Janzen, *Diam. Relat. Mater.* **6**, 1297 (1997).